

# Laboratory Determination of Parameters for Transversely Anisotropic Model of Stiff Clay

Monika ČERNÍKOVÁ<sup>a,1</sup>, Martin KRUPÍČKA<sup>a</sup>, Tomáš MOHYLA<sup>a</sup>, Jan BOHÁČ<sup>a</sup>,  
Josef ROTT<sup>a</sup> and David MAŠÍN<sup>a</sup>

<sup>a</sup>*Charles University in Prague, Faculty of Science, Albertov 6, 12843 Prague, Czech Republic*

**Abstract.** The overconsolidated Brno clay (Tegel) was subjected to the extensive laboratory testing. The obtained data were used in the anisotropic hypoplastic model and a backanalysis of coefficient of earth pressure at rest  $K_0$  was performed. The resulting value of  $K_0 = 0.75$  was not estimated by more conventional methods.

**Keywords.** Anisotropy, backanalysis, in-situ stress, stiff clay, tunnelling

## 1. Introduction

The recently opened urban inner ring road of the town of Brno (Czech Republic) includes the Královo Pole Tunnels, consisting of two mostly parallel tunnel tubes with a separation distance of about 70 m and the length of approximately 1250 m. The height and width of the cross section are about 11.5 m and 14 m, respectively, and the overburden thickness varies from 6 m to 21 m. The tunnels have been built in the developed urban environment and mostly, except for the portal portions, in the strata of high plasticity Neogene (Miocene) clay, called Tegel (Figure 1).

The tunnels have been driven by the New Austrian Tunelling Method. The face of one of the tunnels included the geometry of two exploratory galleries of a triangular cross-section with arched sides, constructed as a part of the geotechnical site investigation. The width and height of the galleries reached 4.75 m and 4.5 m, respectively. The primary lining of the galleries consisted of 0.10 m of sprayed concrete in combination with steel profiles.

To estimate the horizontal stresses in the clay massif four unsupported circular side drifts of the diameter of 1.9 m were excavated from the exploratory galleries. The convergences of these cylindrical cavities were measured during the site investigation [1] and a coefficient of earth pressure at rest  $K_0$  in overconsolidated Tegel was back-calculated.

In backanalysing the final tunnel, galleries, and the side drifts the recently developed hypoplastic model for clay was used, which included stiffness anisotropy [2]. The basic set of the parameters for the hypoplastic model for clays, as well as the additional parameters for the enhanced model, were determined using the laboratory experiments.

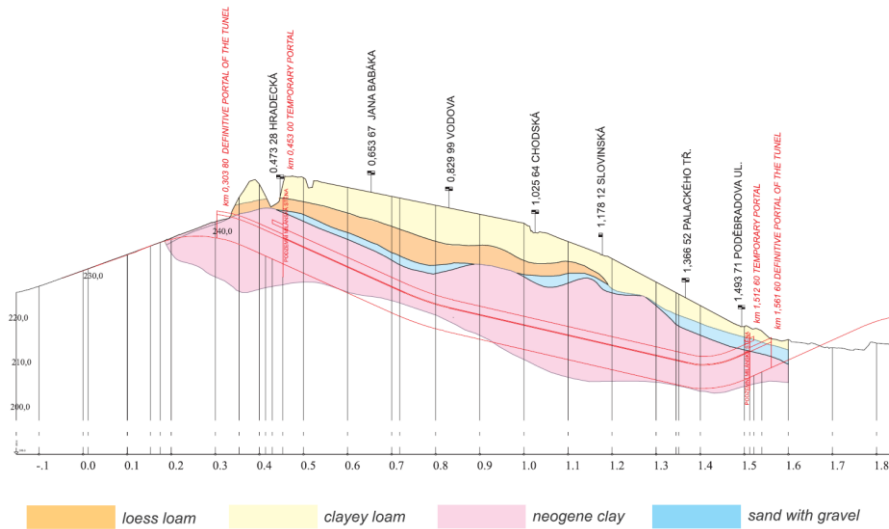


Figure 1. Longitudinal geological cross-section along the tunnels [1].

## 2. Brno Tegel

The Miocene Brno Tegel was deposited in the Carpathian Fore-deep, north of the Vienna Basin. The area was strongly influenced by tectonic phenomena, which controlled the depths of the Neogene sea, and therefore the height of the clayey sediments varied.

In Pliocene and Quaternary periods erosion of the marine sediments took place. However the depth of the erosion has not been determined to date. From the geotechnical viewpoint the clay exhibits moderate apparent overconsolidation, with yield stress ratio (apparent overconsolidation ratio OCR) reaching ca 10. However it has not been explained to date, whether the apparent OCR was caused by mechanical unloading (erosion) or by ageing.

The Tegel is a calcareous clay, of grey-blue to grey-green colour, the upper parts, down to 15 to 20 metres, brownish due to weathering. Often there are crystals of calcite and/or limonite. Crystals of gypsum are frequent especially in the upper brown layers, their occurrence diminishing in the grey layers. Locally the clay can be sandy.

The Tegel sedimented in the marine environment and during its subsequent exposure it was subject to intense chemical changes, especially due to freshwater leaching. This might explain the intense fissuring, reported typically in site investigations: The percolation of fresh water is concentrated into pre-existing tectonic cracks. The resulting chemical changes, formation of gypsum, calcite (10-34%) and limonite, were most intense in the zones. Assuming that the chemical changes were accompanied by volume changes, the fissuring may have originated in a similar way like freezing and shrinkage [3].

Table 1 summarizes the mineralogical composition of the three clay samples. The analyses were carried out by X-ray diffraction. The typical grading curve is shown in Figure 2, and index properties summarized in Table 2.

**Table 1.** X-ray diffraction analysis from Brno-Slatina.

| Depth (m) | Quartz (%) | Calcite (%) | Smectite (%) | Kaolinite (%) | Muscovite (%) |
|-----------|------------|-------------|--------------|---------------|---------------|
| 24        | 27         | 29          | 15           | 3             | 8             |
| 27        | 33         | 34          | 0            | 10            | 7             |
| 36        | 23         | 31          | 7            | 7             | 26            |

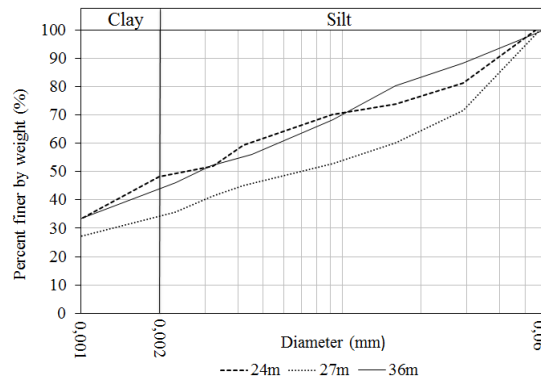


**Figure 2.** Grading curves of Brno Tegel.

**Table 2.** Index properties of Brno Tegel.

| Depth (m) | Liquid Limit (%) | Plastic Limit (%) | Plasticity Index (%) | Colloidal Activity (%) |
|-----------|------------------|-------------------|----------------------|------------------------|
| 24        | 56               | 31                | 25                   | 0,515                  |
| 27        | 40               | 30                | 10                   | 0,289                  |
| 36        | 61               | 35                | 26                   | 0,577                  |

### 3. Laboratory Determination of Parameters of Brno Tegel

Undisturbed samples were taken by an open thin-walled steel sampler of the inner diameter of 114 mm, manufactured to the DIN specification [4]. Undisturbed and reconstituted specimens were tested in the oedometer, triaxial, and shear box apparatuses.

#### 3.1. Strength

The critical state strength was determined using

- Conventional triaxial reconstituted specimens;
- Frictionless triaxial reconstituted specimens;
- Translational and ring shear box.

The stress paths and the failure line produced by the triaxial tests (CIUP) of reconstituted specimens with frictionless platens are shown in Figure 3. CIUP triaxial tests on undisturbed specimens of 38 mm diameter were used in calibrating the 'large-strain' shear stiffness. The stress paths and the calibration are in Figure 4.

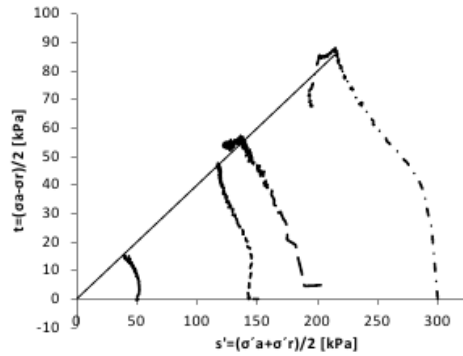


**Figure 3.** Stress paths of CIUP of reconstituted specimens with frictionless platens [5].

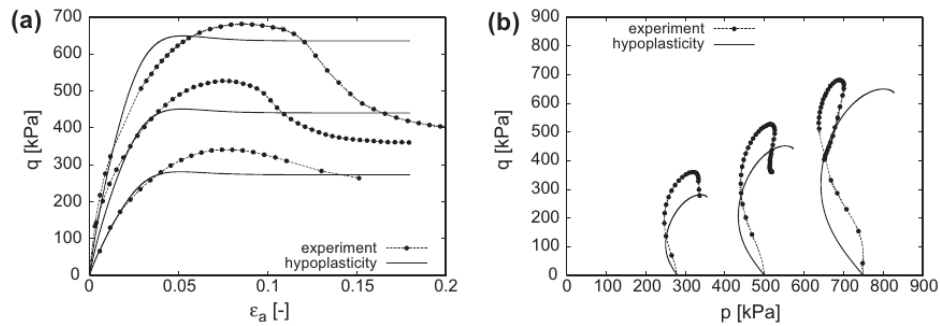


**Figure 4.** Triaxial CIUP Stress paths and calibration of undisturbed specimens using the 'basic' hypoplastic model ( $p$  is the effective mean stress; [6]).

Further to triaxial testing the critical state friction angle  $\varphi_c$  was also estimated by testing reconstituted specimens in direct shear. Both the translational and the ring shear devices were used (see Table 3). There are many rather conflicting theoretical and experimental findings about the possibility of reaching the critical state of soils in the ring shear, or in simple shear (e.g. [7, 8, 9], and many others). It seems that ring shear tests underestimate the critical state friction angle. Nevertheless it was used in the current project as a quick estimate of critical state friction angle  $\varphi_c$ .

**Table 3.** The critical state friction angle  $\varphi_c$  [°] of Brno Tegel.

| Test Series              | Triaxial<br>Conventional Platens | Triaxial<br>Frictionless Platens | Ring Shear<br>(Bromhead Type) |
|--------------------------|----------------------------------|----------------------------------|-------------------------------|
| Feda et al., 1995 [3]    | 27.5°                            | -                                | -                             |
| Svoboda et al., 2010 [6] | 18.9°                            | -                                | 19.9°                         |
| Fencl, 2012 [5]          | 21.0°                            | 23.6°                            | 19.8°                         |

### 3.2. 1-D Compressibility

The compressibility of Tegel was studied using oedometer testing of both undisturbed and reconstituted specimens up to the vertical effective stresses of 13 MPa. The

intrinsic and sedimentation compression lines, and the compression curves of undisturbed specimens normalized using the void index [10] can be seen in Figure 5.

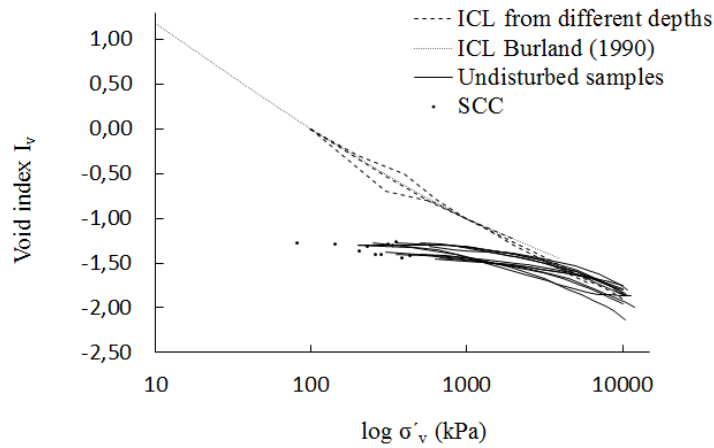


**Figure 5.** Normalized compression curves of Brno Tegel.

The quasi-preconsolidation pressures were determined from the compressibility curves by Casagrande's method. The obtained values at individual depths of sampling are shown in Figure 6.

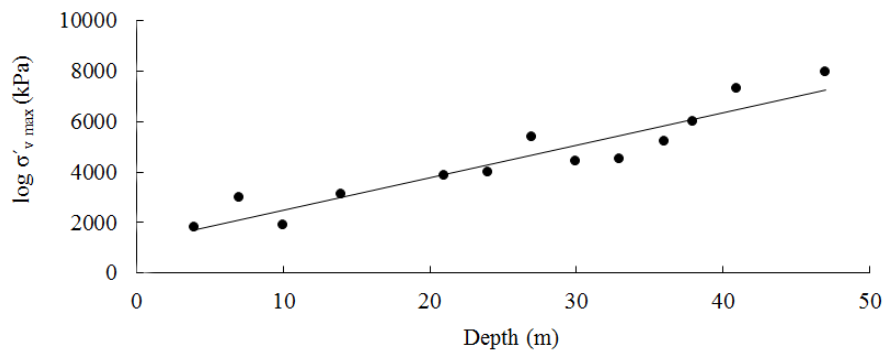


**Figure 6.** The profile of quasi-preconsolidation pressures  $\sigma'_{vmax}$ .

### 3.3. Small and Very Small Strains – Stiffness Anisotropy of Tegel

The model for cross-anisotropic stiffness requires five further model parameters  $G_{tp0}$ ,  $\alpha_G$ ,  $\chi_{Gv}$ ,  $\chi_{GE}$ ,  $\nu_{pp0}$  (the index  $t$  denotes the transverse direction to the plane of isotropy – the vertical direction, while  $p$  represents the in-plane direction – the horizontal direction; [11]). In the model the very small strain shear modulus  $G_{tp0}$  requires two

parameters  $A_g$  and  $n_g$ . Their values have been determined using bender element results [6].

The small strain stiffness was measured using submersible LVDTs mounted on the conventional triaxial undisturbed specimens. The main anisotropy parameter  $\alpha_G = G_{pp0}/G_{tp0}$  was estimated from the measurements of vertically transmitted shear wave velocities through two specimens. The first one trimmed vertically, the second one horizontally. The experiments were carried out under all-round effective cell pressure corresponding to the estimated in-situ mean effective stress. As shown in [11], stiff to hard clays exhibit just mild stress-induced anisotropy, and therefore the isotropic stress state during the bender elements testing was not expected to influence the results significantly. Average of times of arrival at frequencies 3,5,7,9 kHz was used to evaluate the shear wave velocity. These frequencies showed no effect of the overshooting phenomenon. The measured  $G_{pp0}$  was consistently higher than  $G_{tp0}$  (Figure 7a). To quantify  $\alpha_G$  the data were fitted by a straight line (Figure 7a). The resulting coefficient  $\alpha_G \approx 1.45$  is shown in Figure 7b.

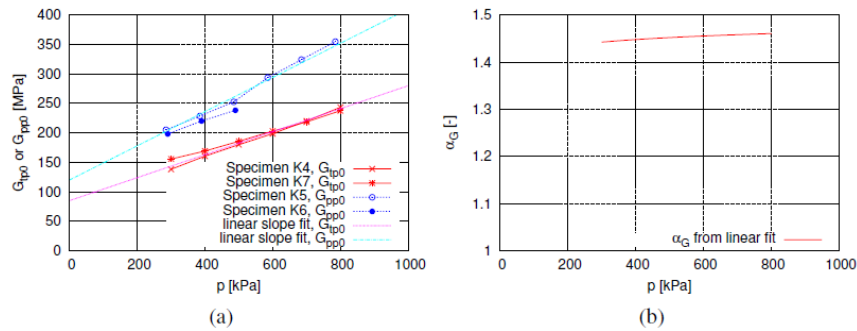


**Figure 7.** Shear moduli obtained by bender element measurements (a) and the resulting coefficient  $\alpha_G$  (b).

The remaining anisotropy parameters were quantified using small isotropic probes, and constant radial stress shearing probes, applied to the triaxial undisturbed specimens. Again the specimens were first isotropically consolidated to estimated in-situ stresses. Submersible LVDTs were mounted on the specimens in two pairs: two measuring the axial, and two measuring the radial strains during the probes ( $\epsilon_a$  and  $\epsilon_r$ , respectively). The strains obtained from the radial LVDTs were supplemented by the  $\epsilon_r$  computed from the conventional measurements of volume changes using usual 'flow pumps' (volume-pressure controllers). The radial strains during the  $\sigma_r = \text{const}$  shearing probes were negligible, as indicated by both local measurements and by radial strains computed from the volume changes (Figure 8a). In Figure 8b there are results of the isotropic probes, which were approximated by a linear fit  $\epsilon_r = 0.6 \epsilon_a$ .

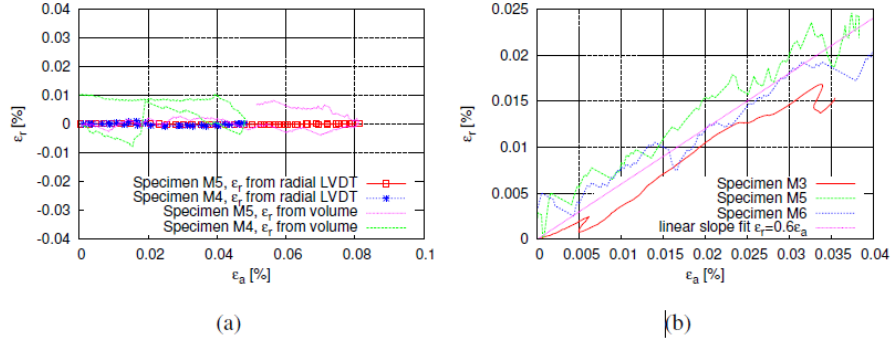


**Figure 8.** Axial ( $\epsilon_a$ ) and radial ( $\epsilon_r$ ) strains obtained by shearing (a) and isotropic (b) stress probing of undisturbed triaxial specimens.

From the compliance matrix for transversely isotropic soil, for constant radial stress probes it follows that  $v_{tp0}$  is directly proportional to the radial strain rate [12]. Negligible radial strains of Figure 8(a) therefore imply  $v_{tp0} \approx 0$ . For the isotropic probes it then follows for  $E_{h0}/E_{v0} \equiv \alpha_E = \delta\epsilon_a/\delta\epsilon_r$ , ( $\delta\epsilon$  means strain rate). Therefore for the experimentally found  $\epsilon_r = 0.6 \epsilon_a$  (Figure 8b)  $\alpha_E \approx 1.67$ .  $\alpha_G \approx 1.45$  from the bender elements measurements (Figure 7b) then yields  $x_{GE} \approx 0.73$ , which is close to  $x_{GE} \approx 0.8$  suggested by Mašin and Rott [11] on the basis of the experimental database from the literature.

#### 4. The Full Set of Parameters and the Use in Numerical Model

The parameters for transversely anisotropic hypoplastic model, which were determined and calibrated on laboratory tests, are listed in Table 4.

**Table 4.** Parameters for transversely anisotropic hypoplastic model.

| Parameter   | Parameter              | Parameter  | Parameter   |
|-------------|------------------------|------------|-------------|
| $\gamma$    | 18.8 kNm <sup>-3</sup> | $\chi$     | 0.8         |
| $\phi_c$    | $\sim 22^\circ$        | $\nu$      | 0.33        |
| $\lambda^*$ | 0.128                  | $A_g$      | 5300 kPa    |
| $\kappa^*$  | 0.015                  | $n_g$      | 0.50        |
| $N$         | 1.5                    | $v_{tp0}$  | $\sim 0.00$ |
| $R$         | 0.0001                 | $\alpha_G$ | 1.45        |
| $m_{rat}$   | 0.5                    | $x_{GE}$   | 0.73        |
| $\beta_r$   | 0.2                    | $x_{Gv}$   | (1.0)       |

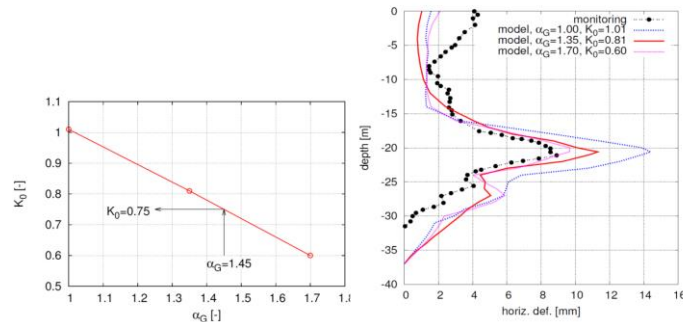


**Figure 9.** Value of  $K_0$  (a) and horizontal displacement (b) in the vicinity of exploratory adit [12].

To obtain the relation between the shear moduli ratio  $\alpha_G = G_{pp0}/G_{tp0}$  and  $K_0$ , three pairs of  $\alpha_G$ - $K_0$  were backcalculated in such a manner that horizontal and vertical convergence ratio  $u_h / u_v = 1.25$ , measured in the monitoring, was obtained. The values of  $\alpha_G = 1,00$ ; 1,35 and 1,70 were based on literature review.  $K_0 = 0.75$  can be deduced with laboratory determined value of  $\alpha_G = 1.45$  (Figure 9a). The simulations of horizontal displacements agree well with the monitoring data (Figure 9b).

## 5. Conclusions

The soil parameters for transversely anisotropic model have been calibrated using the oedometer and triaxial tests on undisturbed and reconstituted specimens. The numerical simulations based on the presented laboratory testing successfully back-calculated the in-situ monitoring data, and also enabled us to estimate with reasonable confidence the at-rest coefficient  $K_0$ , which for the pseudo-overconsolidated clay in question proved impossible to be determined by other direct or indirect methods.

## References

- [1] J. Pavlík, L. Klímek and D. Rupp, Geotechnical exploration for the Dobrovského tunnel, the most significant structure on the large city ring road in Brno. *Tunel 13* (2004), No 2, 2-12.
- [2] D. Mašín, Clay hypoplasticity model including stiffness anisotropy. *Géotechnique 64* (2014), No. 3, 232-238.
- [3] J. Feda, J. Boháč, and I. Herle, Shear resistance of fissured Neogene clays. *Engineering Geology 39*, (1995), 171-184.
- [4] DIN 4021 Aufschluss durch Schürfe und Bohrungen sowie Entnahme von Proben (Exploration by excavation and borings, sampling – in German), DIN, Oktober 1990.
- [5] M. Fencel, Critical state strength of Brno Clay (in Czech), MSc Thesis, Charles University in Prague, (2012), 64 pp.
- [6] T. Svoboda, D. Mašín and J. Boháč, Class A predictions of a NATM tunnel in stiff clay. *Computers and Geotechnics 37* (2010), No. 6, 817-825.
- [7] A. Sadrekarimi and S.M. Olson, Critical state friction angle of sands. *Géotechnique 61* (2011), No 9, 771-783.
- [8] J.H. Atkinson, W.H.W. Lau and J.J.M. Powell, Measurements of soil strength in simple shear test. *Can. Geotech. J.* 28 (1991), 255-262.
- [9] D.W. Airy and D.M. Wood, An evaluation of direct simple shear tests on clay. *Géotechnique 37* (1987), No 1, 25-35.
- [10] J.B. Burland, ON the compressibility and shear strength of natural clays. *Géotechnique 40* (1990), No 3, 329-378.
- [11] D. Mašín and J. Rott, Small strain stiffness anisotropy of natural sedimentary clays: review and a model. *Acta Geotechnica 9* (2014), 299-312.
- [12] J. Rott, D. Mašín, J. Boháč, M. Krupička and T. Mohyla, Evaluation of  $K_0$  of stiff clay by back-analysis of convergence measurements from unsupported cylindrical cavity. Submitted to *Acta Geotechnica*.